

1

Research Article

2 Mapping and validation of sex-linked SNP markers in the
3 swimming crab *Portunus trituberculatus*

4

5 Ronghua Li^{a,b,c,1}, Michaël Bekaert^{c,1}, Junkai Lu^{a,b}, Shaokun Lu^{a,b}, Zhouyi Zhang^a,
6 Weijia Zhang^a, Ouwen Shi^a, Chen Chen^a, Changkao Mu^{a,b}, Weiwei Song^{a,b}, Herve
7 Migaud^{a,b,c,*} and Chunlin Wang^{a,b,*}

8

9 ^a Key Laboratory of Applied Marine Biotechnology, Ministry of Education, Ningbo
10 University, Ningbo 315211, China

11 ^b Collaborative Innovation Center for Zhejiang Marine High-efficiency and Healthy
12 Aquaculture, Ningbo University, Ningbo 315211, China

13 ^c Institute of Aquaculture, Faculty of Natural Sciences, University of Stirling, Stirling
14 FK9 4LA, Scotland, United Kingdom

15

16

17 * Corresponding author.

18 *E-mail address*: herve.migaud@stir.ac.uk (H. Migaud); wangchunlin@nbu.edu.cn (C.
19 Wang).

20 ¹ These authors contributed equally to this work.

21

22

23

24

25 **Abstract**

26 *Portunus trituberculatus* is one of the most commercially important marine crustacean
27 species for both aquaculture and fisheries in Southeast and East Asia. Production of
28 monosex female stocks is attractive in commercial production since females are more
29 profitable than their male counterparts. Identification and mapping of the sex-linked
30 locus is an efficient way to elucidate the mechanisms of sex determination in the
31 species and support the development of protocols for monosex female production. In
32 this study, a sex-averaged map and two sex-specific genetic maps were constructed
33 based on 2b-restriction site-associated DNA sequencing. A total of 6,349 genetic
34 markers were assigned to 53 linkage groups. Little difference was observed in the
35 pattern of sex-specific recombination between females and males. Association
36 analysis and linkage mapping identified 7 markers strongly associated with sex, four
37 of which were successfully mapped on the extremity of linkage group 22. Females
38 were homozygous and males were heterozygous for those 7 markers strongly
39 suggesting an XX/XY sex determination system in this species. Three Markers were
40 successfully validated in a wild population of *P. trituberculatus* and exhibited a
41 specificity ranging from 93.3% to 100%. A high-resolution melting based assay was
42 developed for sex genotyping. This study provides new knowledge and tools for sex
43 identification which will help the development of protocols for monosex female
44 production of *P. trituberculatus* and support future genomic studies.

45

46 **Keywords:** genetic linkage map, sex marker, sex determination, QTL mapping, high-
47 resolution melting (HRM)

48

49

50 **Highlights**

- 51 • A genome survey and restriction site-associated DNA sequencing were
52 combined.
- 53 • A high-density genetic map was created with 53 linkage groups.
- 54 • XX/XY sex determination system was validated.
- 55 • Male-specific alleles were identified and validated for 7 SNP markers.
- 56 • A PCR-based genetic sex identification method was successfully validated.
- 57
- 58

59 Introduction

60 The swimming crab, *Portunus trituberculatus*, naturally distributed along the coastal
61 waters of temperate western Pacific Ocean, is a commercially important marine
62 crustacean species for both aquaculture and fisheries in East Asian countries. In
63 China, the farming of *P. trituberculatus* developed quickly and reached a production
64 of 116,251 tons in 2018 (Fisheries Bureau of Ministry of Agriculture, 2019). Despite
65 the growing commercial interest in this species, research effort has been limited so far
66 with recent literature focused on the species biology including ovarian development
67 (Che et al., 2018; Liu et al., 2018), larviculture (Shi et al., 2019), population genetics
68 (Liu et al., 2012), genomics of growth traits (Lv et al., 2017; Feng et al., 2018),
69 nutrition (DHA/EPA, Hu et al., 2017; phospholipids, Song et al., 2019) and immune
70 function (Ren et al., 2017; Wu et al., 2019).

71 Sexual dimorphisms, especially in growth rates, between female and male individuals
72 have been reported in many aquaculture species, making the production of monosex
73 stocks particularly attractive for the aquaculture industry (Scott et al., 1989; Budd et
74 al., 2015). Sexual dimorphisms has also been reported in *P. trituberculatus* with
75 female crabs exhibiting higher growth rate and greater body weight (Wang et al.,
76 2018). In addition, female crabs that reached sexual maturation are more profitable
77 with a higher market value due to the accumulation of vitellogenin in the ovary.
78 However, no protocol is available for the production of monosex females and the
79 identification of sex in *P. trituberculatus* seedlings is difficult and can only be done
80 reliably after 3-4 months of culture in ponds based on the shape of the abdomen.
81 Therefore, in culture, male crabs are usually removed continuously during the
82 growing period and female kept until harvest. This “sex grading” method is labour-
83 intensive and very inefficient. The use of monosex female juveniles would greatly
84 improve productivity and profitability of the sector. However, the prerequisites to any
85 animal monosexing methodologies are the elucidation of the species sex
86 determination system and the identification of potential sex-associated markers. These
87 would help to fast track the establishment of all-female *P. trituberculatus*.

88 Linkage mapping and association mapping are two major strategies to identify genetic
89 loci and markers for traits of commercial interest (Yu et al., 2017). The combination
90 of high-throughput sequencing (HTS) and restriction digestion enzymes enable the

91 rapid discovery of genome-wide genetic markers, facilitating the construction of high-
92 density genetic linkage maps and sex-specific quantitative trait loci (QTL) mapping,
93 which narrow down the sex-determining region and can provide useful sex-linked
94 markers (Palaiokostas et al., 2013a, 2013b; Cui et al., 2015; Palaiokostas et al., 2015;
95 Yu et al., 2017; Shi et al., 2018; Waiho et al., 2019; Wang et al., 2019). Recently, a
96 high-density linkage map based on specific length amplified fragment sequencing
97 (SLAF-seq) has been constructed for *P. trituberculatus*, in which 10 growth-related
98 QTLs and a significant QTL for sex were identified (Lv et al., 2017, 2018). This
99 provided valuable genomic resources that can be used for marker-assisted selection
100 and breeding, however, the candidate sex-specific markers identified were not
101 completely linked (Lv et al., 2018). More detailed studies are required to identify
102 informative markers associated with sex in *P. trituberculatus*.

103 In the present study, a genome survey was first conducted to provide basic
104 characteristics of *P. trituberculatus* genome to be used as a reference for the following
105 marker validation. Then, 2b-restriction site-associated DNA (2b-RAD) sequencing
106 was employed to construct a high-density genetic linkage map and association
107 analysis of sex-related QTL for *P. trituberculatus*. Finally, new sex-linked markers
108 were validated based on the genome survey analysis aiming at increasing the
109 reliability and accuracy of sex identification and elucidating the sex determination
110 system in *P. trituberculatus*. Overall, the new knowledge gained will help the
111 development of monosexing protocols in the species and support the expansion of the
112 swimming crab aquaculture.

113

114

115 Materials and Methods

116 **Genome sequencing survey and analysis**

117 Genomic DNA of one female *P. trituberculatus* collected from wild population of
118 Zhejiang Province, China was extracted from muscle for genome survey analysis (low
119 coverage, whole genome sequencing). Two libraries with insert size of 350
120 nucleotides were constructed from randomly fragmented genomic DNA. The
121 construction, sequencing and assembly of the genome survey libraries were
122 performed by Novogene Co. (Beijing, China). Sequencing was performed on an
123 Illumina HiSeq 2500 sequencing platform with paired-end 150 bp reads. Reads of low
124 quality (*i.e.* with an average quality score less than 20) or having ambiguous bases or
125 adaptors were clipped using Trimmomatic v0.38 (Bolger et al., 2014) as standard
126 pre-processing methods. Jellyfish v2.2.10 (Marçais and Kingsford, 2011) was used for
127 K-mer and the genome size estimation. SOAPdenovo r241 (Luo et al., 2012) was used
128 for the *de novo* genome assembly. Due to the low coverage, no annotation was
129 pursued, but completeness of the gene captured was assessed using BUSCO v3
130 (Waterhouse et al., 2018) using the Metazoa dataset. Reads were deposited at the EBI
131 European Nucleotide Archive (ENA) projects PRJEB32999.

132

133 **Mapping family preparation and sample collection for QTL analysis**

134 An F1 full-sib family for linkage map construction was created by two parents from
135 the wild population of Zhejiang Province, China. The full-sib family was reared at
136 XinYi Aquatic Products Limited Company in 2015. A total of 118 progenies were
137 randomly selected after being reared for 4 months. Muscle tissue (claw) from both
138 parents and 118 offspring were collected and preserved in 95% ethanol until DNA
139 extraction.

140 Muscle tissues of an additional 30 wild individuals (15 males and 15 females) from
141 the Zhejiang Province, China were collected for the QTL mapping. Genomic DNA
142 was extracted from the above samples using a standard phenol/chloroform protocol.

143

144 **Library preparation and sequencing**

145 The construction of 2b-RAD library using *Bsa*XI restriction enzymes was performed
146 and sequenced by Oebiotech Co., Ltd. (Shanghai, China) following the methodology
147 proposed by Wang *et al.* (2012, 2016) and using the multiplexing structure detailed in
148 Supplementary Table S2. Reads were deposited at the EBI European Nucleotide
149 Archive (ENA) projects PRJNA371532 (family cross) and PRJEB32947 (wild
150 animals).

151

152 **Genotyping 2b-RAD alleles**

153 The 2b-RAD sequence data from the 150 individuals (120 full-sib family with
154 parents, and 30 wild individuals; Table S1) were pre-processed to discard low quality
155 reads (*i.e.* with a quality score less than 20), missing tag structure or ambiguous bases.
156 The clean reads were demultiplexed (Table S2) as described in Wang *et al.* (2016).
157 Six offspring from the full-sib family (9, 25, 26, 65, 73, 75) were found to have
158 substantially lower quality reads and were excluded from all further analyses.
159 Resulting reads were assembled *de novo*, sorted into loci and genotypes using Stacks
160 v2.3 (Catchen *et al.*, 2013). The key parameter values employed were: a minimum
161 stack depth of 6, a maximum of 2 mismatches allowed in a locus in an individual and
162 up to 1 mismatch between loci when building the catalogue. Informative markers
163 were kept only when presenting at least two alleles with a minor allele frequency
164 (MAF) above 0.01 and were present in at least 75% of the samples. Only one SNP
165 was reported.

166

167 **Construction of the linkage maps**

168 Based on the SNP alleles obtained, a linkage map was constructed with LepMap3
169 (Rastas, 2017). SNPs deviating from the expected Mendelian segregation ($P < 0.001$)
170 were excluded. Based on available karyotyping data (Zhu *et al.*, 2005), the number of
171 linkage groups was set to 53 (logarithm of odds, LOD = 9). The total length of the
172 map in centimorgans (cM) was estimated using Kosambi mapping functions. Maps
173 generated with OrderMarker2 module were checked for contiguous sequence (contig)
174 continuity. Data processing was automatised using scripts available from

175 <https://github.com/pseudogene/radmap>. Genetic maps were drawn using Genetic-
176 Mapper v0.11 (Bekaert, 2016). Recombination rates were calculated using Lepmap3
177 output as the number of recombination event divided by the total number of
178 individuals for each chromosome for each sex class.

179

180 **Identification and validation of sex associated markers**

181 Using the phenotypic gender data from 30 wild individuals and parents of the full-sib
182 family, an association analysis was performed within the package R/SNPassoc v1.9-2
183 (González et al., 2007), using the "codominant" model for the QTL analysis. The
184 sequences of the predicted sex associated markers from QTL results were aligned
185 against scaffold of genome survey database using Blast+ v2.8.1 (Altschul et al.,
186 1990). Primers were designed on flanking regions of the SNPs using the Primer3
187 v2.40 (Untergasser et al., 2012).

188 Muscles from an extra 60 wild adult *P. trituberculatus* (30 males, 30 females) were
189 collected from Xiangshan, Zhejiang Province, China, for the validation of these
190 predicted sex associated markers. Genomic DNA was extracted from the muscle
191 tissue by using a genomic DNA extraction kit (BioTeke, Beijing, China) following
192 the manufacturer protocols. Polymerase chain reaction (PCR) was performed in 10 µL
193 volumes containing 2× Power Taq PCR Master Mix (BioTeke, Beijing, China) 5 µL,
194 1 µM of each primer set, and about 100 ng template DNA. PCR was performed on a
195 Master-cycler gradient thermal cycler (Eppendorf) with the following program: 3 min
196 at 94 °C; 35 cycles of 1 min at 94 °C, annealing for 1 min, 72 °C for 1 min per cycle;
197 followed by 5 min at 72 °C. PCR products were sequenced in both directions on the
198 ABI3730 platform (Applied Biosystems). Alignment of the sequenced fragments was
199 performed using Vector NTI 10.0 (Invitrogen, Carlsbad, CA) for the confirmation of
200 predicted SNPs. High-resolution melting (HRM) analysis was also applied to the
201 discrimination of predicted sex associated SNPs. PCR amplification and HRM
202 analysis were performed on a LightCycler®480 real-time PCR instrument (Roche
203 Diagnostics) as previously described (Chen et al., 2018).

204

205 **Results**

206 **Genome survey summary**

207 From the two 350 bp short paired-end DNA libraries constructed for the genome
208 survey analysis of *P. trituberculatus*, a total of 165,950,266 raw paired-end reads
209 were generated by sequencing. After removing low quality and adapters, 157,193,348
210 paired-end reads remained (94.7%). The estimated genome size using SOAPdenovo
211 K-mer module (K = 17) was 1.083 Gb (Fig. 1A) with high heterozygosity (1.02%). A
212 relatively high percentage of repetitive sequences (58.50%) was detected in the
213 *P. trituberculatus* genome (Table 1). After assembly of this genome survey with
214 SOAPdenovo (K = 41), a total of 1,910,434 scaffolds were generated with N50 of
215 1,212 nt, for a total length of 892,095,304 nt with a GC-value of 42.02% (Table 1),
216 and 81.4% BUSCO metazoa genes were at least partially recovered (Fig. 1B).

217

218 **2b-RAD data analysis and SNP calling**

219 High throughput sequencing of the 150 animals produced 253,650,280 paired-end
220 reads in total (two runs). After the removal of low-quality (QC < 20) and incomplete
221 reads, 75.5% of the total reads were retained (191,576,072 paired-end reads).
222 Demultiplexing generated 957,880,360 sequences with a length of 27 bp. The
223 sequences were assembled *de novo* and genotypes for all samples were obtained using
224 Stacks, yielding 496,426 unique SNP loci. Average coverage of each loci was 18.5×,
225 92.5× and 27.3× for offspring, parents and wild population, respectively. A total of
226 48,862 loci were polymorphic-allelic markers shared by at least 75% of the samples
227 with a minor allele frequency above 0.01. All of these markers were subsequently
228 used to construct genetic linkage maps and to perform an association analysis.

229

230 **High-density linkage map construction**

231 Using genotype information from the 48,862 loci of the 114 individuals (112
232 offspring and 2 parents), sex-averaged, female, and male genetic linkage maps were
233 constructed with LepMap3 at the LOD threshold of 9.0 (Table 2 and Table S3 & S4).
234 The maps were constructed using 6,349 informative SNPs to 53 linkage groups (each

235 comprising at least 10 SNPs), spanning a total distance of 2,960.5 cM, 2,728.3 cM,
236 3,237.7 cM for sex-averaged, female, and male map respectively (Fig. 2 and Fig. S1
237 & S2). The average marker interval of the sex-averaged map is 0.47 cM. The male-
238 specific linkage map is slightly longer than the female-specific map with an average
239 male to female ratio of 1.19. The sex-specific recombination was studied, and little
240 difference was observed in the recombination rates between sex, with the average
241 female/male ratio of 0.97 over all the linkage groups (linkage group 46-52 were
242 excluded from the recombination calculations because of low marker numbers).

243

244 **QTL mapping and validation of sex associated markers**

245 Using both the 48,862 informative markers and 6,349 mapped markers, R/SNPassoc
246 was used to conduct a quantitative trait locus (QTL) mapping analysis for the sex
247 determination association. A total of 7 markers strongly associated with sex (100%
248 specificity, Table 3) were identified, four of which were successfully mapped on the
249 extremity of LG 22, where a highly significant QTL for gender (Fig. 3A, peak
250 LOD = 8.48, at the whole genomic level) was located in the region ranging from
251 4.874 to 6.201 cM (Fig. 3B) suggested to be a potential sex determining region.
252 Females were homozygous and males were heterozygous for those 7 markers. The 2b-
253 RAD sequences and the scaffold sequences of all these 7 markers identified from the
254 survey database were provided in Table S5. Orthologous sequences of these scaffolds
255 were searched in the GenBank through NCBI BLAST (Johnson et al., 2008),
256 however, no hits were detected.

257 Primers were designed for the seven potential sex-specific markers according to the
258 corresponding scaffolds of the genome survey, and validated in another wild
259 population (30 males, 30 females). Three of them were successfully amplified (Table
260 4), two of which were located in the genetic linkage map (Ptr67655, Ptr138136).
261 Sequencing results demonstrated that the specificity of these 3 markers in the
262 discrimination of the wild population were 93.3%, 100% and 100%, respectively for
263 markers PS7, PS8 and PS11 (Table 5). Interestingly, more than one SNP was found in
264 PS11, and the predicted male-specific SNP (C/T) appeared to be C in all the 60
265 individuals, but six new SNPs in this fragment were detected, females were
266 homozygous and males were heterozygous for these six new SNPs.

267 All three markers were tested using HRM analysis to develop a sex genotyping assay.
268 Only primer set PS11 was found to be clearly distinct between sex in the melting
269 profiles from the HRM analysis (Fig. 4) and T_m calling analysis showed that the
270 melting points were 80.5 °C and 81.9 °C, respectively for male and female.

271

272 Discussion

273 High-density genetic linkage maps are important genomic tools for fine mapping of
274 quantitative trait loci, genome assembly, functional gene localization, comparative
275 genome and analysis of sex chromosome evolution. The 2b-RAD technology has been
276 widely applied for the construction of high-density linkage maps in many aquaculture
277 species due to its relative simplicity (no requirement for prior genomic data), cost-
278 effectiveness, even distribution on the genomes, uniform fragments and adjustable
279 genome coverage (Shi et al., 2014; Cui et al., 2015; Tian et al., 2015; Feng et al.,
280 2018; Liu et al., 2018; Wang et al., 2018). In the present study, three genetic linkage
281 maps were constructed for *P. trituberculatus* using 2b-RAD, covering a total distance
282 of 2,960.5 cM, 2,728.3 cM and 3,237.7 cM for sex-averaged, female, and male maps,
283 respectively. The average marker interval of the sex-averaged map was 0.47 cM,
284 which was comparable to previous reports in many crustacean species (0.4 -1.51 cM),
285 including *Litopenaeus vannamei* (0.7 cM, Yu et al., 2015); *Penaeus monodon*
286 (1.51 cM, Guo et al., 2019); *Scylla paramamosain* (0.81 - 0.92 cM, Waiho et al.,
287 2019; Zhao et al., 2019); *Eriocheir sinensis* (0.49 - 0.81 cM, Cui et al., 2015; Qiu et
288 al., 2017) and *P. trituberculatus* (0.51 cM, Lv et al., 2017). The high resolution of the
289 new SNP-based linkage map will facilitate further studies of detailed QTL mapping.

290 Monosex populations in aquatic animals are generally produced by combining sex
291 reversal and progeny testing. The ability to determine rapidly the genetic sex of an
292 individual through sex-linked markers can fast track the development of monosex
293 lines in economically important cultured species (Chen et al., 2007). In the present
294 study, association analysis and linkage mapping identified 7 markers strongly
295 associated with sex, four of which were successfully mapped onto the extremity of
296 LG 22, where a significant QTL for gender (peak LOD = 8.48, at the whole genomic
297 level) was located in the region ranging from 4.874 to 6.201 cM. Females were
298 homozygous and males were heterozygous for those 7 markers confirming the
299 suggested XY sex determination system of *P. trituberculatus* (Lv et al., 2018). All the

300 scaffolds containing the 7 sex-linked markers were further searched against GenBank
301 to identify candidate gene(s) for sex determination, however, no informative blast hits
302 were detected. Therefore, it is possible that these sex-linked loci found in
303 *P. trituberculatus* represent novel genes or regulatory elements. Further studies are
304 needed to characterise the function of these new sex-specific loci.

305 Chromosomal karyotype analysis showed that the diploid chromosome number of
306 *P. trituberculatus* is 106 ($2n = 106$), however, no heteromorphism has been observed
307 for sex chromosomes (Zhu et al., 2005). Sex chromosomes are derived from ordinary
308 autosomes, which is thought to involve recombination suppression in sex determining
309 regions, followed by the accumulation of deleterious mutations and the degeneration
310 of the sex-specific (*e.g.* Y) chromosome (Graves, 2006). It is generally thought that
311 the morphological differentiation between sex chromosomes is a by-product of the
312 degeneration of the chromosome that is present only in the heterogametic sex (*i.e.* Y
313 or W) and is thus completely sheltered from genetic recombination (Bachtrog, 2006).

314 In our study, there was little difference in the recombination rates between sex, with
315 an average female/male ratio of 0.97, recombination suppression has not been
316 detected in any specific linkage groups (including LG 22 where the sex-determining
317 region is located). The lack of non-recombining regions together with the apparent
318 existence of a sex-determining region may suggest "proto-sex chromosomes" in
319 *P. trituberculatus*. In such a sex determination system, a chromosome carries a newly
320 arisen sex-determining gene or a newly evolved sex-determining region, but
321 recombination suppression has not yet evolved and therefore there is no sex
322 chromosome heteromorphism (Charlesworth and Mank, 2010).

323 Validation of the 3 successfully amplified sex associated markers in another wild
324 population of *P. trituberculatus* exhibited a specificity from 93.3% to 100%. Only
325 markers Ptr138136 (primer set PS8) and Ptr62530 (primer set PS11) were strongly
326 associated with sex. This is especially true for the latter locus (Ptr62530) in which the
327 predicted SNP (C/T) appeared to be C in all individuals screened from the validation
328 population, however, six new SNPs in this fragment were also found to be associated
329 with sex which could also be easily separated by HRM analysis. The inconsistency of
330 identified sex-linked markers in different populations has also been reported in
331 previous species including *L. vannamei* and *P. trituberculatus* (Yu et al., 2017; Lv et
332 al., 2018). This may be partly explained by the lack of recombination suppression in
333 regions that include and flank the sex determining mutation in these species, so that

334 the detected sex associated markers may frequently cross over during meiosis.
335 Nevertheless, the marker Ptr138136 (primer set PS8) was found to be strongly
336 associated with sex in both populations of *P. trituberculatus*, and it was mapped to the
337 most significant sex associated region in the LG 22 with a peak LOD of 8.48.
338 Although marker Ptr62530 was not located on the genetic map, it was also found to be
339 linked with sex. The combination of these sex associated markers should significantly
340 improve the reliability and accuracy of sex identification in *P. trituberculatus*.

341 The confirmation of the sex-determining region and system will greatly help further
342 studies to search for sex-determining genes and apply molecular sexing methods of
343 *P. trituberculatus* while also benefitting developmental and evolutionary biology
344 fields. Diverse sex determination systems have evolved in the animal and plant
345 kingdoms, including the genetic sex determination (GSD), the environmental sex
346 determination (ESD) especially with regards to temperature (TSD), and the
347 interaction between the two (Korpelainen, 1990; Charlesworth and Mank, 2010;
348 Palaiokostas et al., 2013a). In fish, the complex interaction between genetic and
349 environmental factors has been observed in several species such as Nile tilapia,
350 *Oreochromis niloticus* (Cáceres et al., 2019), sea bass, *Dicentrarchus labrax* (Piferrer
351 et al., 2005) and flatfish species (Luckenbach et al., 2009), with male/female
352 heterozygous system (XX/XY or ZZ/ZW). Sex determination in crustacea can also
353 show plasticity, being influenced by environmental variables such as light and
354 temperature (Ford, 2008). Despite the male heterozygous system shown in
355 *P. trituberculatus*, the influence of environmental variables on sex determination can
356 not be ruled out and should be investigated.

357 The genome survey performed in the present study provides useful background for the
358 species given the lack of whole-genome resources. In our study, the 2b-RAD library
359 generated tags with 27 bp in length, which was short to design primers for PCR
360 validation or function analysis. However, after blasting against the genome survey
361 data, the 7 potential sex-specific markers identified matched a significant scaffold
362 sequence extending the flanking region for primer design and PCR validation.
363 Besides, a BUSCO completeness assessment of *P. trituberculatus* genome survey
364 recovered 81.4% of the metazoa genes, which confirmed the overall robustness of the
365 sequencing and assembly of the genome survey, providing valuable resources for
366 future genetic studies in this species. Genome survey could also estimate some basic
367 genomic characteristics which can then help to determine the best sequencing

368 strategies and most suitable assembly algorithms for whole genome studies. The
369 estimated genome size of *P. trituberculatus* in our study was 1.083 Gb with high
370 heterozygosity (1.02%), and a relatively high percentage of repetitive sequences
371 (58.50%) detected. The complexity of crustacean genomes has been acknowledged
372 previously and it makes the assembly of the whole genome sequence challenging
373 when only based on data generated by Illumina sequencing (Yu et al., 2015; Lv et al.,
374 2017). Future sequencing efforts for crustacean species with such a complex genomes
375 should integrate other advanced technology such as the PacBio long reads sequencing
376 platform and algorithms to reduce assembly errors.

377

378 Ethical statement

379 This study was approved by the Ethics Committee of Ningbo University, and
380 conducted according to relevant national and international guidelines.

381

382 Author Contributions

383 Conceptualization, R.L. and C.L.; Methodology, R.L. and M.B.; Formal analysis,
384 M.B., R.L. and H.M.; Investigation, J.L., S.L., Z.Z., W.Z., O.S., C.C., C.M. and W.S.;
385 Writing - original draft preparation, R.L. and M.B.; Writing - review and editing,
386 funding acquisition, R.L., C.W. and H.M.

387

388 Acknowledgments

389 This research was supported by National Key R&D Program of China
390 (2018YFD0900303), National Key R&D Program of China (2018YFD0901304),
391 Natural Science Foundation of Zhejiang Province (No. LY17C190005, No.
392 LY18H110003), Ministry of Agriculture of China & China Agriculture Research
393 System (no: CARS-48), Ningbo Science and Technology Project (2017C110007),
394 CSC Scholarship (201708330421) and K.C. Wong Magana Fund in Ningbo
395 University.

396

397 References

- 398 Altschul, S.F., Gish, W., Miller, W., Myers, E.W., Lipman, D.J., 1990. Basic local
399 alignment search tool. *Journal of Molecular Biology* 215, 403–410.
400 [https://doi.org/10.1016/S0022-2836\(05\)80360-2](https://doi.org/10.1016/S0022-2836(05)80360-2)
- 401 Bachtrog, D., 2006. A dynamic view of sex chromosome evolution. *Current Opinion*
402 *in Genetics and Development* 16, 578–585.
403 <https://doi.org/10.1016/j.gde.2006.10.007>
- 404 Bekaert, M., 2016. Genetic-Mapper: vectorial genetic map drawer. *F1000Research* 5.
405 <https://doi.org/10.7490/f1000research.1112266.1>
- 406 Bolger, A.M., Lohse, M., Usadel, B., 2014. Trimmomatic: A flexible trimmer for
407 Illumina sequence data. *Bioinformatics* 30, 2114–2120.
408 <https://doi.org/10.1093/bioinformatics/btu170>
- 409 Budd, A., Banh, Q., Domingos, J., Jerry, D., 2015. Sex control in fish: approaches,
410 challenges and opportunities for aquaculture. *Journal of Marine Science and*
411 *Engineering* 3, 329–355. <https://doi.org/10.3390/jmse3020329>
- 412 Cáceres, G., López, M.E., Cádiz, M.I., Yoshida, G.M., Jedlicki, A., Palma-Véjares,
413 R., Travisany, D., Díaz-Domínguez, D., Maass, A., Lhorente, J.P., Soto, J.,
414 Salas, D., Yáñez, J.M., 2019. Fine mapping using whole-genome sequencing
415 confirms anti-Müllerian hormone as a major gene for sex determination in
416 farmed Nile Tilapia (*Oreochromis niloticus* L.). *G3 (Bethesda, Md.)* 9, 3213–
417 3223. <https://doi.org/10.1534/g3.119.400297>
- 418 Catchen, J., Hohenlohe, P.A., Bassham, S., Amores, A., Cresko, W.A., 2013. Stacks:
419 An analysis tool set for population genomics. *Molecular Ecology* 22, 3124–3140.
420 <https://doi.org/10.1111/mec.12354>
- 421 Charlesworth, D., Mank, J.E., 2010. The birds and the bees and the flowers and the
422 trees: Lessons from genetic mapping of sex determination in plants and animals.
423 *Genetics* 186, 9–31. <https://doi.org/10.1534/genetics.110.117697>
- 424 Che, J., Liu, M., Dong, Z., Hou, W., Pan, G., Wu, X., 2018. The growth and ovarian
425 development pattern of pond-reared swimming crab *Portunus trituberculatus*.
426 *Journal of Shellfish Research* 37(3), 521–528.
- 427 Chen, S.L., Li, J., Deng, S.P., Tian, Y.S., Wang, Q.Y., Zhuang, Z.M., Sha, Z.X., Xu,
428 J.Y., 2007. Isolation of female-specific AFLP markers and molecular

429 identification of genetic sex in half-smooth tongue sole (*Cynoglossus*
430 *semilaevis*). *Marine Biotechnology* 9, 273–280. [https://doi.org/10.1007/s10126-](https://doi.org/10.1007/s10126-006-6081-x)
431 006-6081-x

432 Chen, X., Li, R., Wang, C., Mu, C., Song, W., Liu, L., Shi, C., Zhan, P., 2018. An
433 effective method for identification of three mussel species and their hybrids
434 based on SNPs. *Conservation Genetics Resources*.
435 <https://doi.org/10.1007/s12686-018-1051-y>

436 Cui, Z., Hui, M., Liu, Y., Song, C., Li, X., Li, Y., Liu, L., Shi, G., Wang, S., Li, F.,
437 Zhang, X., Liu, C., Xiang, J., Chu, K.H., 2015. High-density linkage mapping
438 aided by transcriptomics documents ZW sex determination system in the Chinese
439 mitten crab *Eriocheir sinensis*. *Heredity* 115, 206–215.
440 <https://doi.org/10.1038/hdy.2015.26>

441 Feng, X., Yu, X., Fu, B., Wang, X., Liu, H., Pang, M., Tong, J., 2018. A high-
442 resolution genetic linkage map and QTL fine mapping for growth-related traits
443 and sex in the Yangtze River common carp (*Cyprinus carpio haematopterus*).
444 *BMC Genomics* 19, 1–13. <https://doi.org/10.1186/s12864-018-4613-1>

445 Fisheries Bureau of Ministry of Agriculture, 2019. China fishery statistical yearbook.
446 China Agriculture Press, Beijing, China.

447 Ford, A.T., 2008. Can you feminise a crustacean? *Aquatic Toxicology* 88, 316–321.
448 <https://doi.org/10.1016/j.aquatox.2008.04.013>

449 González, J.R., Armengol, L., Solé, X., Guinó, E., Mercader, J.M., Estivill, X.,
450 Moreno, V., 2007. SNPAssoc: an R package to perform whole genome
451 association studies. *Bioinformatics* 23, 644–645.
452 <https://doi.org/10.1093/bioinformatics/btm025>

453 Graves, J.A.M., 2006. Sex chromosome specialization and degeneration in mammals.
454 *Cell* 124, 901–914. <https://doi.org/10.1016/j.cell.2006.02.024>

455 Guo, L., Xu, Y.-H., Zhang, N., Zhou, F.-L., Huang, J.-H., Liu, B.-S., Jiang, S.-G.,
456 Zhang, D.-C., 2019. A high-density genetic linkage map and QTL mapping for
457 sex in black tiger shrimp (*Penaeus monodon*). *Frontiers in Genetics* 10, 1–9.
458 <https://doi.org/10.3389/fgene.2019.00326>

459 Hu, S., Wang, J., Han, T., Li, X., Jiang, Y., Wang, C., 2017. Effects of dietary
460 DHA/EPA ratios on growth performance, survival and fatty acid composition of
461 juvenile swimming crab (*Portunus trituberculatus*). *Aquaculture Research* 48,
462 1291–1301. <https://doi.org/10.1111/are.12971>

463 Johnson, M., Zaretskaya, I., Raytselis, Y., Merezhuk, Y., McGinnis, S., Madden, T.L.,
464 2008. NCBI BLAST: a better web interface. *Nucleic acids research* 36, 5–9.
465 <https://doi.org/10.1093/nar/gkn201>

466 Korpelainen, H., 1990. Sex ratios and conditions required for environmental sex
467 determination in animals. *Biological Reviews of the Cambridge Philosophical*
468 *Society* 65, 147–184. <https://doi.org/10.1111/j.1469-185x.1990.tb01187.x>

469 Liu, H., Pang, M., Yu, X., Zhou, Y., Tong, J., Fu, B., 2018. Sex-specific markers
470 developed by next-generation sequencing confirmed an XX/XY sex
471 determination system in bighead carp (*Hypophthalmichthys nobilis*) and silver
472 carp (*Hypophthalmichthys molitrix*). *DNA Research* 25, 257–264.
473 <https://doi.org/10.1093/dnares/dsx054>

474 Liu, L., Li, J., Liu, P., Zhao, F., Gao, B., Du, Y., 2012. A genetic linkage map of
475 swimming crab (*Portunus trituberculatus*) based on SSR and AFLP markers.
476 *Aquaculture* 344–349, 66–81. <https://doi.org/10.1016/j.aquaculture.2012.01.034>

477 Liu, M., Pan, J., Liu, Z., Cheng, Y., Gong, J., Wu, X., 2018. Effect of estradiol on
478 vitellogenesis and oocyte development of female swimming crab, *Portunus*
479 *trituberculatus*. *Aquaculture* 486, 240–245.
480 <https://doi.org/10.1016/j.aquaculture.2017.12.034>

481 Luckenbach, J.A., Borski, R.J., Daniels, H. V., Godwin, J., 2009. Sex determination
482 in flatfishes: Mechanisms and environmental influences. *Seminars in Cell and*
483 *Developmental Biology* 20, 256–263.
484 <https://doi.org/10.1016/j.semcdb.2008.12.002>

485 Luo, R., Liu, B., Xie, Y., Li, Z., Huang, W., Yuan, J., He, G., Chen, Y., Pan, Q., Liu,
486 Yunjie, Tang, J., Wu, G., Zhang, H., Shi, Y., Liu, Yong, Yu, C., Wang, B., Lu,
487 Y., Han, C., Cheung, D.W., Yiu, S.-M., Peng, S., Xiaoqian, Z., Liu, G., Liao, X.,
488 Li, Y., Yang, H., Wang, Jian, Lam, T.-W., Wang, Jun, 2012. SOAPdenovo2: an
489 empirically improved memory-efficient short-read de novo assembler.
490 *GigaScience* 1, 18. <https://doi.org/10.1186/2047-217X-1-18>

491 Lv, J., Gao, B., Liu, P., Li, J., Meng, X., 2017. Linkage mapping aided by de novo
492 genome and transcriptome assembly in *Portunus trituberculatus*: applications in
493 growth-related QTL and gene identification. *Scientific Reports* 7, 1–13.
494 <https://doi.org/10.1038/s41598-017-08256-8>

495 Lv, J., Sun, D., Huan, P., Song, L., Liu, P., Li, J., 2018. QTL mapping and marker
496 identification for sex-determining: Indicating XY sex determination system in

497 the swimming crab (*Portunus trituberculatus*). *Frontiers in Genetics* 9, 1–9.
498 <https://doi.org/10.3389/fgene.2018.00337>

499 Marçais, G., Kingsford, C., 2011. A fast, lock-free approach for efficient parallel
500 counting of occurrences of k-mers. *Bioinformatics* 27, 764–770.
501 <https://doi.org/10.1093/bioinformatics/btr011>

502 Palaiokostas, C., Bekaert, M., Davie, A., Cowan, M.E., Oral, M., Taggart, J.B.,
503 Gharbi, K., McAndrew, B.J., Penman, D.J., Migaud, H., 2013a. Mapping the sex
504 determination locus in the Atlantic halibut (*Hippoglossus hippoglossus*) using
505 RAD sequencing. *BMC Genomics* 14, 1–12. [https://doi.org/10.1186/1471-2164-](https://doi.org/10.1186/1471-2164-14-566)
506 14-566

507 Palaiokostas, C., Bekaert, M., Khan, M.G.Q., Taggart, J.B., Gharbi, K., McAndrew,
508 B.J., Penman, D.J., 2015. A novel sex-determining QTL in Nile tilapia
509 (*Oreochromis niloticus*). *BMC Genomics* 16, 1–10.
510 <https://doi.org/10.1186/s12864-015-1383-x>

511 Palaiokostas, C., Bekaert, M., Khan, M.G.Q., Taggart, J.B., Gharbi, K., McAndrew,
512 B.J., Penman, D.J., 2013b. Mapping and Validation of the Major Sex-
513 Determining Region in Nile Tilapia (*Oreochromis niloticus* L.) Using RAD
514 Sequencing. *PLoS ONE* 8, 1–9. <https://doi.org/10.1371/journal.pone.0068389>

515 Piferrer, F., Blázquez, M., Navarro, L., González, A., 2005. Genetic, endocrine, and
516 environmental components of sex determination and differentiation in the
517 European sea bass (*Dicentrarchus labrax* L.). *General and Comparative*
518 *Endocrinology* 142, 102–110.

519 Qiu, G.F., Xiong, L.W., Han, Z.K., Liu, Z.Q., Feng, J. Bin, Wu, X.G., Yan, Y.L.,
520 Shen, H., Huang, L., Chen, L., 2017. A second generation SNP and SSR
521 integrated linkage map and QTL mapping for the Chinese mitten crab *Eriocheir*
522 *sinensis*. *Scientific Reports* 7, 1–11. <https://doi.org/10.1038/srep39826>

523 Rastas, P., 2017. Lep-MAP3: robust linkage mapping even for low-coverage whole
524 genome sequencing data. *Bioinformatics* 33, 3726–3732.
525 <https://doi.org/10.1093/bioinformatics/btx494>

526 Ren, X., Gao, B., Liu, X., Li, J., Liu, P., 2017. Comparison of immune responses and
527 antioxidant status of different generations of growth-selected *Portunus*
528 *trituberculatus* families. *Aquaculture Research* 48, 1315–1326.
529 <https://doi.org/10.1111/are.12973>

530 Scott, A.G., Penman, D.J., Beardmore, J.A., Skibinski, D.O.F., 1989. The “YY”
531 supermale in *Oreochromis niloticus* (L.) and its potential in aquaculture.
532 *Aquaculture* 78, 3–4.

533 Shi, X., Waiho, K., Li, X., Ikhwanuddin, M., Miao, G., Lin, F., Zhang, Y., Li, S.,
534 Zheng, H., Liu, W., Aweya, J.J., Azmie, G., Baylon, J.C., Quintio, E.T., Ma, H.,
535 2018. Female-specific SNP markers provide insights into a WZ/ZZ sex
536 determination system for mud crabs *Scylla paramamosain*, *S. tranquebarica* and
537 *S. serrata* with a rapid method for genetic sex identification. *BMC Genomics* 19,
538 1–12. <https://doi.org/10.1186/s12864-018-5380-8>

539 Shi, Y., Wang, S., Gu, Z., Lv, J., Zhan, X., Yu, C., Bao, Z., Wang, A., 2014. High-
540 density single nucleotide polymorphisms linkage and quantitative trait locus
541 mapping of the pearl oyster, *Pinctada fucata martensii* Dunker. *Aquaculture* 434,
542 376–384. <https://doi.org/10.1016/j.aquaculture.2014.08.044>

543 Song, D., Shi, B., Ding, L., Jin, M., Sun, P., Jiao, L., Zhou, Q., 2019. Regulation of
544 dietary phospholipids on growth performance, antioxidant activities,
545 phospholipid metabolism and vitellogenesis in prereproductive phase of female
546 swimming crabs, *Portunus trituberculatus*. *Aquaculture* 511, 734230.
547 <https://doi.org/10.1016/j.aquaculture.2019.734230>

548 Tian, M., Li, Y., Jing, J., Mu, C., Du, H., Dou, J., Mao, J., Li, X., Jiao, W., Wang, Y.,
549 Hu, X., Wang, S., Wang, R., Bao, Z., 2015. Construction of a high-density
550 genetic map and quantitative trait locus mapping in the sea cucumber
551 *Apostichopus japonicus*. *Scientific Reports* 5, 1–11.
552 <https://doi.org/10.1038/srep14852>

553 Untergasser, A., Cutcutache, I., Koressaar, T., Ye, J., Faircloth, B.C., Remm, M.,
554 Rozen, S.G., 2012. Primer3—new capabilities and interfaces. *Nucleic Acids*
555 *Research* 40, e115–e115. <https://doi.org/10.1093/nar/gks596>

556 Waiho, K., Shi, X., Fazhan, H., Li, S., Zhang, Y., Zheng, H., Liu, W., Fang, S.,
557 Ikhwanuddin, M., Ma, H., 2019. High-density genetic linkage maps provide
558 novel insights into ZW/ZZ sex determination system and growth performance in
559 mud crab (*Scylla paramamosain*). *Frontiers in Genetics* 10, 1–16.
560 <https://doi.org/10.3389/fgene.2019.00298>

561 Wang, L., Xie, N., Shen, Y., Ye, B., Yue, G.H., Feng, X., 2019. Constructing high-
562 density genetic maps and developing sexing markers in northern snakehead

563 (*Channa argus*). *Marine Biotechnology* 348–358.
564 <https://doi.org/10.1007/s10126-019-09884-z>

565 Wang, S., Liu, P., Lv, J., Li, Y., Cheng, T., Zhang, L., Xia, Y., Sun, H., Hu, X., Bao,
566 Z., 2016. Serial sequencing of isologous RAD tags for cost-efficient genome-
567 wide profiling of genetic and epigenetic variations. *Nature Protocols* 11, 2189–
568 2200. <https://doi.org/10.1038/nprot.2016.133>

569 Wang, S., Meyer, E., McKay, J.K., Matz, M. V., 2012. 2b-RAD: A simple and flexible
570 method for genome-wide genotyping. *Nature Methods* 9, 808–810.
571 <https://doi.org/10.1038/nmeth.2023>

572 Wang, Xinhua, Fu, B., Yu, X., Qu, C., Zhang, Q., Tong, J., 2018. Fine mapping of
573 growth-related quantitative trait loci in Yellow River carp (*Cyprinus carpio*
574 *haematoperus*). *Aquaculture* 484, 277–285.
575 <https://doi.org/10.1016/j.aquaculture.2017.11.016>

576 Wang, X., Wang, Y., Ye, T., Lu, W., Zhou, C., 2018. A preliminary analysis of the
577 growth characteristics of *Portunus trituberculatus*. *Transactions of Oceanology*
578 *and Limnology* 2, 131–136.

579 Waterhouse, R.M., Seppey, M., Simão, F.A., Manni, M., Ioannidis, P., Klioutchnikov,
580 G., Kriventseva, E. V., Zdobnov, E.M., 2018. BUSCO applications from quality
581 assessments to gene prediction and phylogenomics. *Molecular Biology and*
582 *Evolution* 35, 543–548. <https://doi.org/10.1093/molbev/msx319>

583 Wu, X., Huang, Y., Yu, Z., Mu, C., Song, W., Li, R., Liu, L., Ye, Y., Shi, C., Wang,
584 C., 2019. An MBT domain containing anti-lipopolysaccharide factor (PtALF8)
585 from *Portunus trituberculatus* is involved in immune response to bacterial
586 challenge. *Fish and Shellfish Immunology* 84, 252–258.
587 <https://doi.org/10.1016/j.fsi.2018.10.016>

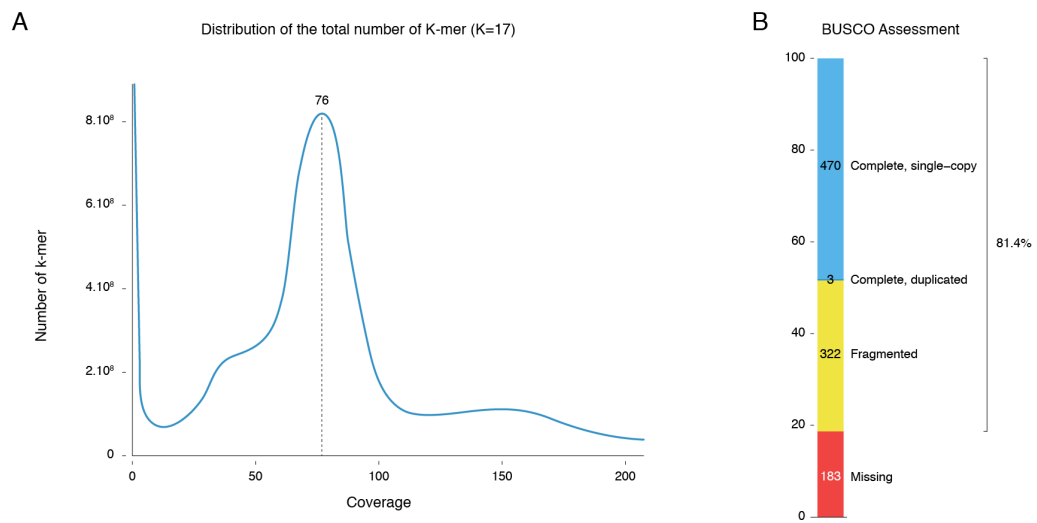
588 Yu, Y., Zhang, X., Yuan, J., Li, F., Chen, X., Zhao, Y., Huang, L., Zheng, H., Xiang,
589 J., 2015. Genome survey and high-density genetic map construction provide
590 genomic and genetic resources for the Pacific White Shrimp *Litopenaeus*
591 *vannamei*. *Scientific Reports* 5, 1–14. <https://doi.org/10.1038/srep15612>

592 Yu, Y., Zhang, X., Yuan, J., Wang, Q., Li, S., Huang, H., Li, F., Xiang, J., 2017.
593 Identification of sex-determining loci in Pacific White Shrimp *Litopenaeus*
594 *vannamei* using linkage and association analysis. *Marine Biotechnology* 19,
595 277–286. <https://doi.org/10.1007/s10126-017-9749-5>

596 Zhao, M., Wang, W., Chen, W., Ma, C., Zhang, F., Jiang, K., Liu, J., Diao, L., Qian,
597 H., Zhao, J., Wang, T., Ma, L., 2019. Genome survey, high-resolution genetic
598 linkage map construction, growth-related quantitative trait locus (QTL)
599 identification and gene location in *Scylla paramamosain*. Scientific Reports 9, 1–
600 10. <https://doi.org/10.1038/s41598-019-39070-z>
601 Zhu, D., Wang, C., Li, Z., 2005. Karyotype analysis on *Portunus trituberculatus*.
602 Journal of Fisheries of China 29(5), 649–653.
603

604 **Figures** (for draft only)

605 **Figure 1** (2 columns – 146 mm x 75 mm)



606

607

Figure 2 (2 columns/full page – 170 mm x 257 mm)

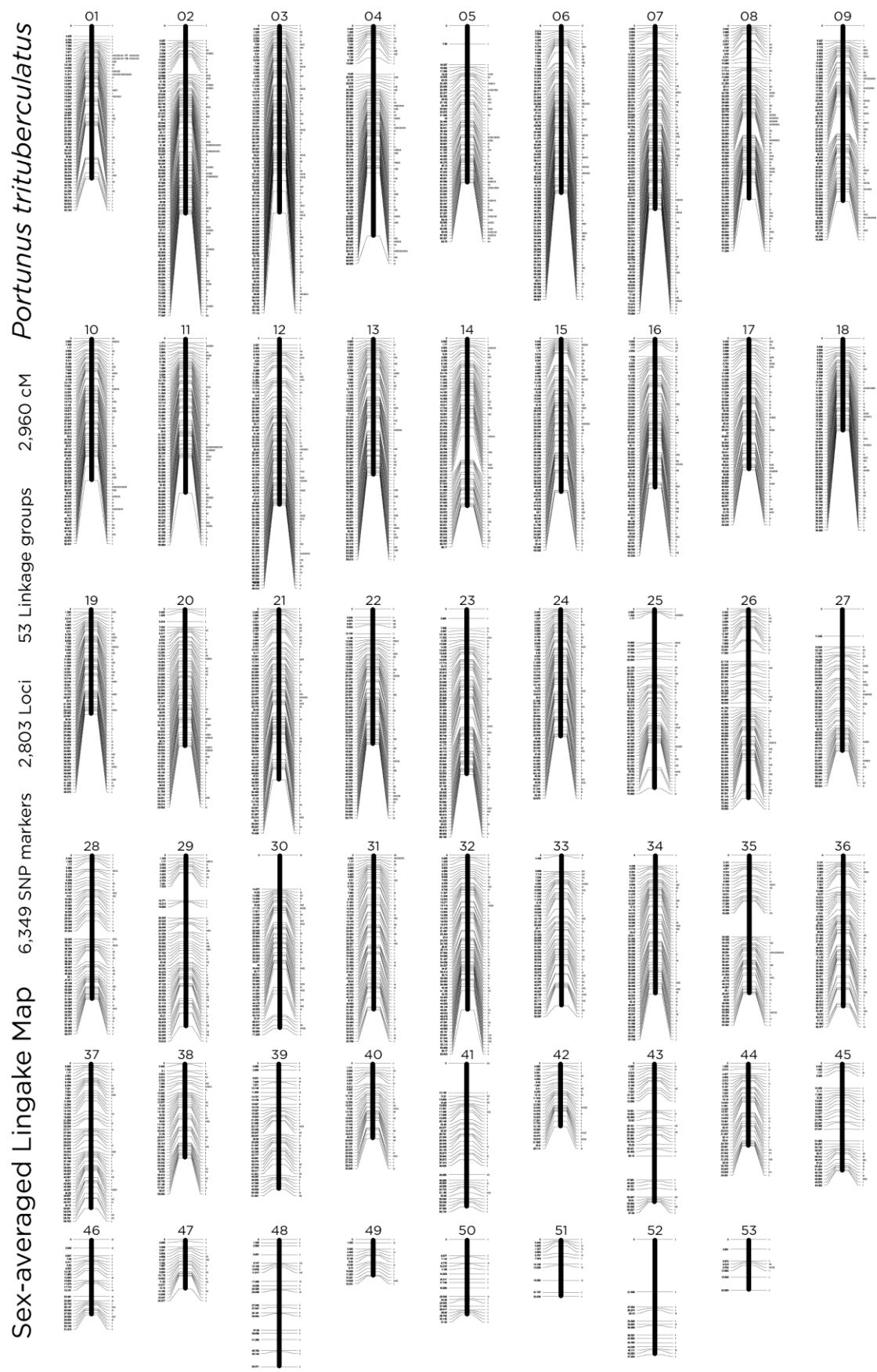
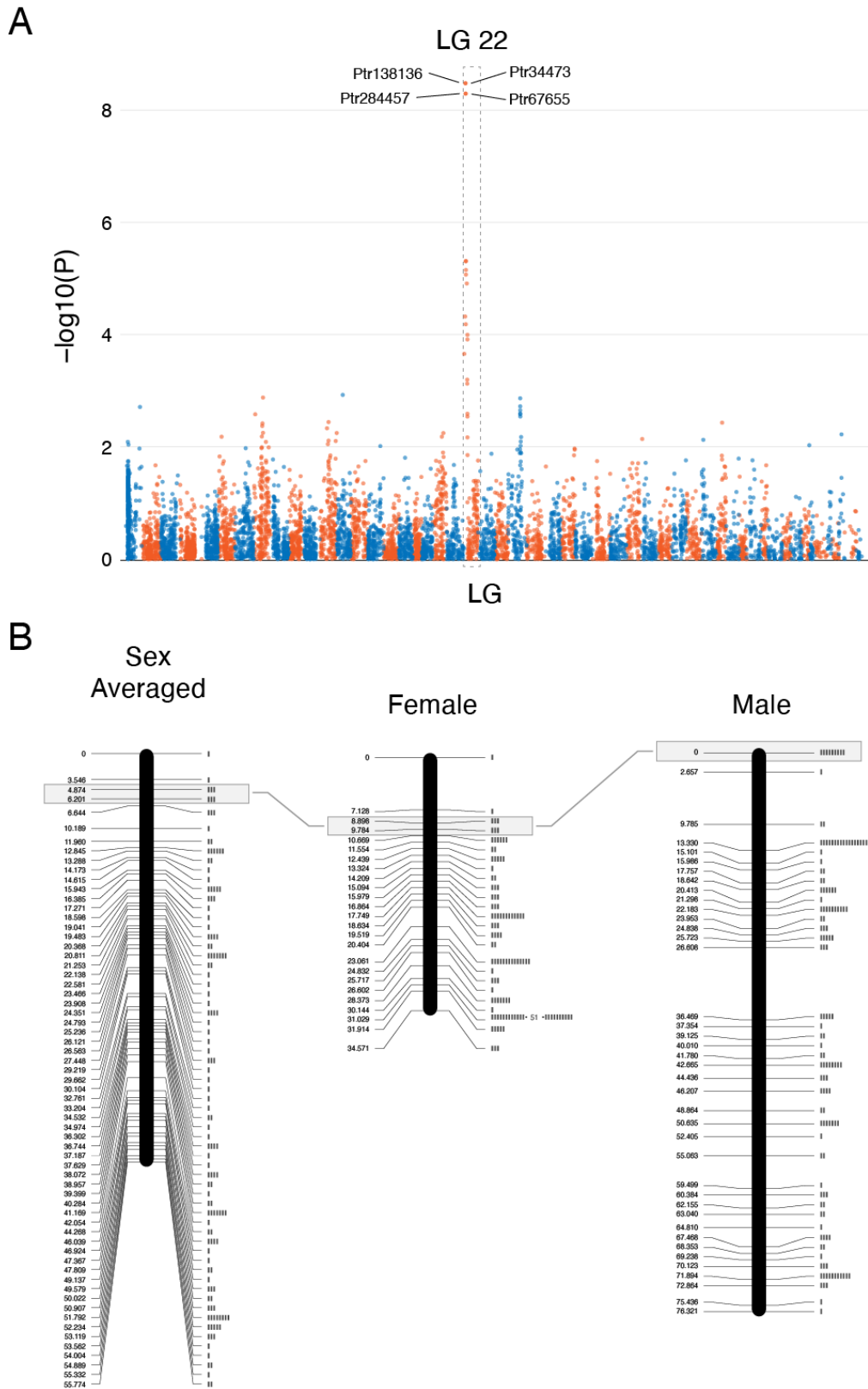
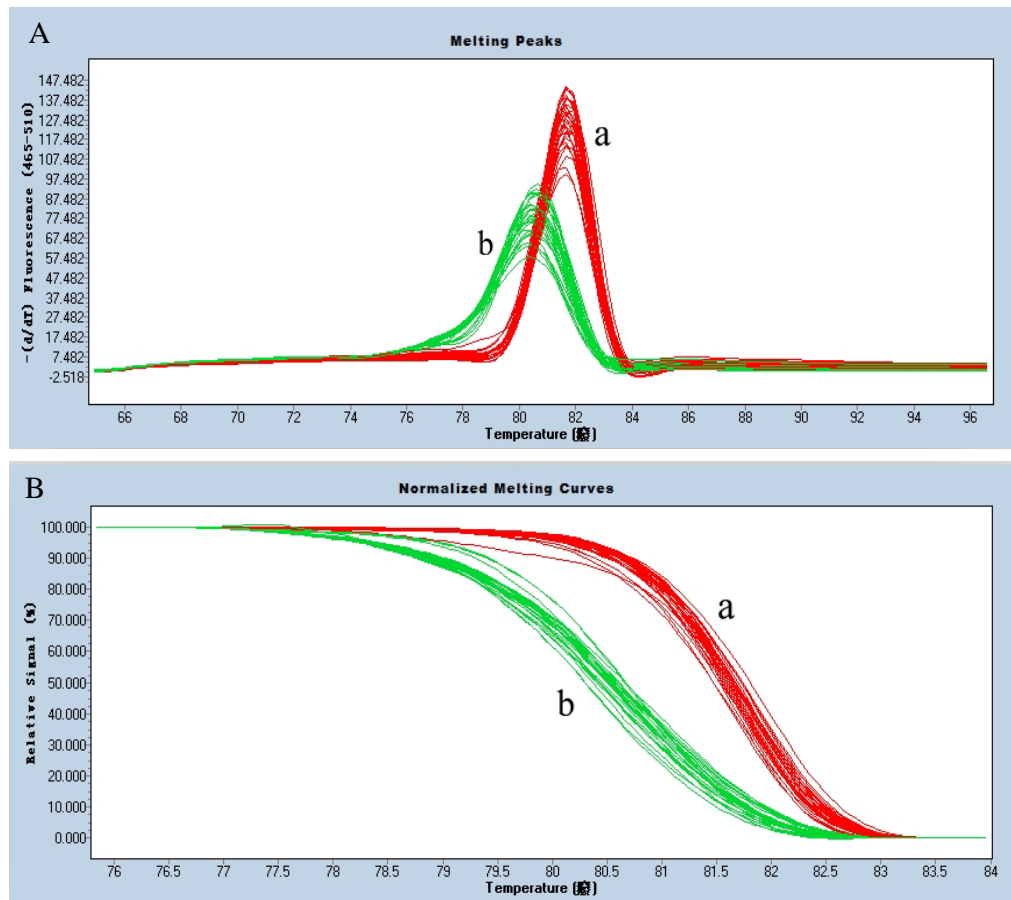


Figure 3 (1 column – 85 mm x 170 mm)



613 **Figure 4**



614

615

616

617

618 **Figure Captions**

619 **Figure 1. Genome coverage.** (A) Distribution of the total number of k-mer analysed.
620 The x-axis is the frequency or the number of times a given k-mer is observed in the
621 sequencing data. The y-axis is the total number of k-mers with a given frequency. The
622 peak is at $K = 76$. (B) BUSCO assessment (Metazoa database; number of BUSCO,
623 978), 81.4% of the genes were recovered.

624

625 **Figure 2. Sex-Averaged linkage map, with linkage groups ordered by number of**
626 **SNP markers.** In each linkage group, numbers shown on the left provide position (in
627 cM) of the respective locus on the chromosome while bars on the right indicates the
628 relative number of SNP markers. Detailed data are provided in Supplementary Data
629 Table S4. Female and Male linkage map are provided in Figure S1 & S2 respectively.

630

631 **Figure 3. Markers associated with phenotypic sex.** (A) Manhattan plot of the
632 association P values for phenotypic sex. The $-\log_{10}(P)$ values for association of
633 directly genotyped SNPs are plotted as a function of position of the genetic map. Each
634 linkage group (LG) has been represented with a different colour. (B) Details of the
635 LG22 and location of the markers associated with phenotypic sex. Female and Male
636 linkage maps are reversed.

637

638 **Figure 4. Discriminations of SNPs between different sex of *P. trituberculatus***
639 **using high-resolution melting analysis for PS11.** (A) Melting peaks. (B)
640 Normalised melting curves. (a) female and (b) male.

641

642 **Tables**

643 **Table 1** – Summary statistics of sequencing and assembly of *P. trituberculatus*
644 genome survey.

645

646

Category	Number/length
Total number of raw PE reads	165,950,266
Maximum read length (nt)	150
Cleaned PE reads	157,193,348
K-mer = 17	83,557,275,304
K-mer = 17 (peak)	76
Estimated genome size	1,083.38 Mb
Estimated repeat	58.50%
Estimated heterozygosity	1.02%
Number of scaffolds	1,910,434
Total length of scaffolds (nt)	892,095,304
Max length of scaffold (nt)	60,585
Scaffold N50 (nt)	1,212
GC value	42.02%
Genome coverage	0.82×

647

648

649 **Table 2** – Summary of the linkage map. Full details for each linkage group in Table
650 S3.

Category	Number/length
Number of linkage group	53
Total markers	6,349
Loci (Sex-averaged)	2,803
Loci (Female)	1,312
Loci (Male)	1,773
Length (Sex-averaged)	2,960.0 cM
Length (Female)	2,728.1 cM
Length (Male)	3,238.1 cM

651

652

653 **Table 3** – SNP markers significantly associated with phenotypic sex. For each marker
 654 the expected association and LOD value are reported. Markers and contig sequences
 655 are provided in Table S5.

Marker ID	LOD	Genetic map location	Genome position	Female	Male
Ptr34473	8.48	22:4.874	contig1099313:1843-1869	A/A	A/G
Ptr62530	8.16	-	contig136081:198-224	T/T	C/T
Ptr84718	7.12	-	contig681633:749-775	C/C	C/T
Ptr138136	8.48	22:4.874	contig 325741:898-872	A/A	A/G
Ptr67655	8.29	22:6.201	contig1070277:1474-1448	T/T	C/T
Ptr284457	8.29	22:4.874	contig569169:778-804	T/T	A/T
Ptr326206	8.16	-	contig1048881:434-460	C/C	C/T

656

657 **Table 4** – Primers used for amplification of the three sex-specific SNP markers.

658 Annealing temperature (T_a): 60°C.

659

Marker ID	Primer ID		Primer sequence
Ptr67655	PS7	Forward	5' -TTAAGTTTGAGTATTGAGTATCCAC- 3'
		Reverse	5' -AATGAGAAGTATTGTAAATGATGTT- 3'
Ptr138136	PS8	Forward	5' -ATACCAGACAAGAGGGCTTC- 3'
		Reverse	5' -TCCCATATAGATATTAGTGTCATTC- 3'
Ptr62530	PS11	Forward	5' -CCGACAACACAGATCCACTAAC- 3'
		Reverse	5' -CGAGTGTGGAGAGAATGATTTTT- 3'

660

661

662 **Table 5** – Validation data of three sex markers in wild populations.

663

Primer ID	Marker ID	Genotype	Male	Female	Specificity (%)
PS7	Ptr67655	A/G	27	1	93.3
		A/A	3	29	
PS8	Ptr138136	T/C	30	0	100.0
		T/T	0	30	
PS11	Ptr62530	T/C A/G C/T A/C C/T T/A	30	0	100.0
		C/C G/G T/T T/T T/T A/A	0	30	

664

665

666 **Supporting information captions**

667 **Table S1. Details of the samples analysed.** (2b-RAD reads numbers, polymorphic
668 marker, and gender are included).

669

670 **Table S2. Demultiplexing key for 2b-RAD library (30 wild individuals).** See
671 Wang *et al.* (Wang et al., 2016) for details on usage.

672

673 **Table S3. Summary statistic of the linkage groups.**

674

675 **Table S4. Details of marker position in the genetic maps.** (A total of 6,349 markers
676 including association with phenotypic sex and marker sequence).

677

678 **Table S5. Details of the 7 sex-linked SNP markers.** Sequence of 2b-RAD and
679 corresponding contig (from genome survey).

680

681 **Figure S1. Female linkage map, with linkage groups ordered by number of SNP
682 markers.**

683

684 **Figure S2. Male linkage map, with linkage groups ordered by number of SNP
685 markers.**

686